



Performance Analysis of H-Darrieus Wind Turbine with NACA0018 and S1046 Aerofoils: Impact of Blade Angle and TSR

Teeab Tahzib¹, Mohammed Abdul Hannan², Yaseen Adnan Ahmed^{1,*}, Iwan Zamil Mustaffa Kamal³

¹ Department of Aeronautical, Automotive and Offshore Engineering, Fakulti Kejuruteraan Mekanikal, Universiti Teknologi Malaysia, 81310 Skudai, Johor, Malaysia

² Faculty of Science, Agriculture and Engineering, Newcastle University, United Kingdom (Singapore campus)

³ Maritime Engineering Technology Section, Universiti Kuala Lumpur Malaysian Institute of Marine Engineering Technology, 32200 Lumut, Perak, Malaysia

ARTICLE INFO

Article history:

Received 1 December 2021

Received in revised form 15 January 2022

Accepted 17 January 2022

Available online 24 January 2022

Keywords:

Vertical Axis Wind Turbine; Darrieus Turbine; TSR; URANS

ABSTRACT

Despite the widespread research and development of HAWTs in recent times, VAWTs are gaining in popularity due to certain critical advantages they provide, for example, wind direction independency. While most existing studies focused on analysing the performance of VAWT using NACA aerofoils, this study compares the performance of NACA0018 and S1046 aerofoil profiles for a range of Speed Ratios (TSRs) and blade pitch angles. It has been found that the S1046 is less sensitive to changes in wind speed, and is thus, a superior choice for urban applications where the wind speed is comparatively low and varies a lot. Three bladed VAWTs of solidity 0.1 was modelled using Solidworks for this study. The CFD simulations were then performed in ANSYS Fluent, utilising the $k-\omega$ SST turbulence model. The model was validated at first before analysing the VAWT performance with the intended aerofoils. Key results indicate that increasing the TSR leads to increases in aerodynamic performances for nearly all cases, and especially so, for lower blade pitch angles. However, this study concludes that VAWT consisting of S1046 aerofoils at -2 degrees of blade pitch and operating at TSR 4 will provide the optimum performance.

1. Introduction

Since the Paris agreement came into force in 2016, research and developments towards sustainable energy harvesting have increased significantly. Wind has always been a reliable source of renewable energy in this regard, and efforts are being devoted to assessing and harvesting both onshore and offshore wind energy [1]. Various methods of harvesting wind energy, both with blades and bladeless; for example, turbine, wingsail, rotating cylinder, kites are being studied as well for quite a long time [2]. However, among the various alternatives, wind turbines, especially vertical or horizontal axis wind turbines, having been found more reliable and efficient, are being widely used these days. For horizontal axis wind turbines, the axis of rotation of the blades is horizontal to the

* Corresponding author.

E-mail address: yaseen@mail.fkm.utm.my (Yaseen Adnan Ahmed)

<https://doi.org/10.37934/cfdl.14.2.1023>

ground. Their blades face the wind perpendicularly and are driven by the lift generated from the wind. For the vertical axis wind turbines on the other hand, the turbine's rotational axis is vertical or perpendicular to the ground.

Despite the extensive application of horizontal axis turbines in recent years, key advantages offered by VAWTs over HAWTs still make them an avenue worthy of further research. Some of those advantages include: VAWTs are omnidirectional and can take the wind from any direction; can be packed more closely in wind farms; produce less noise; have lower centres of gravities due to the majority of their machineries being placed at the ground level and that they offer mechanical simplicity [3,4].

VAWTs are further classified into several types (Figure 1), such as the Savonius, Darrius and hybrid variants. Savonius rotors are propelled by drag, and their mechanism shares similarities to that of simple water wheels. On the other hand, Darrius rotors are lift-driven and achieve much better efficiencies than Savonius, however, come with a lower self-starting capacity [6]. The hybrid type is a combination of the Darrius and Savonius designs and exists to maximise both efficiency and self-starting abilities. Among the Darrius models, the H-Darrius turbine is a popular variant consisting of straight blades, being simpler to manufacture, and needing less maintenance compared to the rest [4].

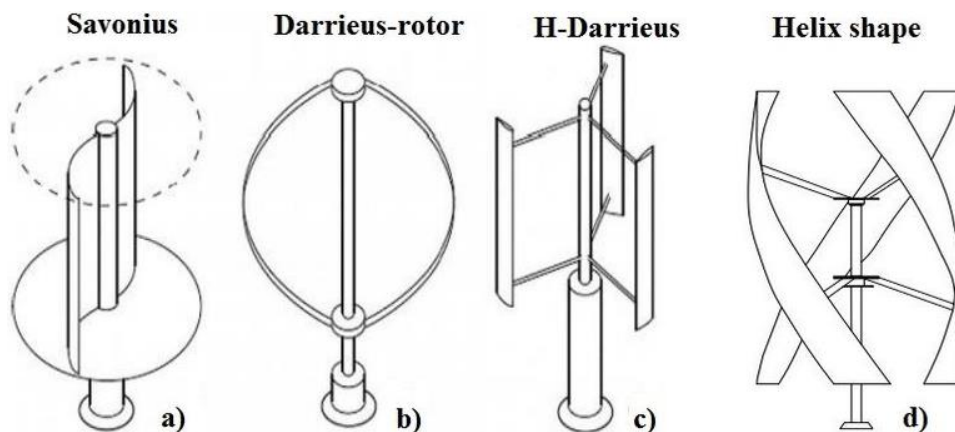


Fig. 1. A few commonly used VAWT shapes [5]

Therefore, significant efforts are being made since the past decade to improve the performance of VAWTs, both through numerical and experimental analysis. CFD, especially turbulence modelling, is extensively used for numerical simulations. However, it is well established that solving turbulent fluctuations in great detail is impractical and unnecessary for many engineering purposes. Thus, rather than solving the unsteady Navier-Stokes equation directly, the Unsteady Reynolds-averaged Navier-Stokes (URANS) equations are used in many simulations, including wind turbines, to save computational time. Some popular URANS turbulence models are the Spalart-Allmaras, $k-\epsilon$, and the $k-\omega$ variants. The main advantage of the $k-\omega$ model is that it does not need wall damping functions for low Reynolds number applications, unlike the $k-\epsilon$ model. However, in itself, the $k-\omega$ model is not adequate for boundary layers with adverse pressure gradients. As such, a hybrid $k-\omega$ SST model is proposed, where the near-wall is modelled with $k-\omega$ and the fully turbulent region further from the wall is modelled with $k-\epsilon$ [7]. These improvements make $k-\omega$ SST the most suitable URANS model to use over zero and adverse pressure gradient boundary layers in external aerodynamics, such as the simulations conducted in this research. Thus, this model is found to capture the 'VAWT's vortex evolution in the dynamic stall' most accurately [8].

The literature available on the simulation of H-Darrius VAWT performance primarily focused on finding the relative velocities and angle of attacks at different tip speed ratios and azimuthal positions, calculation of the ratio of induced to freestream velocity, methods of calculating the normal and tangential forces etc [9-12]. Besides, only few studies were conducted on VAWTs utilising S-series aerofoils at various pitch angles. Table 1 systematically summarizes the scenario, considering some recent papers. From here, it appears that there still remains significant scope for research on optimising the blade pitch angle at different tip speed ratios (to maximise C_p) while also comparing between the performance of NACA and other profile shapes. Therefore, this paper focuses on this research gap and presents a comparative performance analysis between 3-bladed H-Darrius VAWTs utilising NACA 0018 and S-1046 blade profiles, respectively, at various blade pitch angles and tip speed ratios.

Table 1
 Recent advancement in VAWT simulations

Paper title	Brief achievements and limitations
Design of an Offshore Three-Bladed Vertical Axis Wind Turbine for Wind Tunnel Experiments [8]	Studied various NACA and S profiles with different blade numbers, aspect ratio and solidity ratio and concluded that 3 bladed VAWT with S profile provides the best outcome. Did not study the TSR and pitch angle effect.
Aerodynamic performance enhancements of H-rotor Darrieus wind turbine [9]	Used S1046 airfoil and introduced wind-lens to improve the performance. Studied various shapes but did not present any comparison with NACA series and did not study the TSR, solidity and pitch angle effect.
Synergistic analysis of a Darrieus wind turbine using computational fluid dynamics [10]	Conventional NACA 0015 and DU 06-W-200 profiles and non-conventional J-shape blades are studied with wind-lens. Explored different locations of the turbine inside the diffuser, but the effect of TSR, pitch angle etc., are not presented.
Vertical Axis Airborne Wind Turbine: Future of Renewable Energy [11]	Reported a 2D CFD simulation study using three-bladed VAWT placed at different orientations at low wind velocities. Comparisons among various shapes and impacts of TSR, solidity, pitch angle are not explored.

2. Methodology

2.1 Geometric Modelling

2.1.1 VAWT construction

The NACA 0018 and the S1046 aerofoil coordinates from Airfoil Tools [13] are used to model the blades in Solidworks. The design parameters highlighted in Table 2 are used to build the 2D sections of VAWT. Two different VAWT models are developed using NACA and S aerofoil profiles. The developed models are then redefined for subsequent simulations varying only the blade pitch angle. Neither any supporting arm nor the shaft was modelled for any of the simulations. This was a compromise between the extra accuracy they would have provided over the extra meshing complexity and simulation time involved. The solidity of the VAWT is taken as 0.1 for simulations, as it is found to be high enough to allow for smooth VAWT operations at its most effective TSR range and low enough to ‘limit the blade-wake interactions and flow curvature effects’ [14,15].

Table 2
 Design parameters for the two VAWT designs

Parameter	NACA 0018 VAWT	S1046 VAWT
Aerofoil Profile	NACA 0018	S1046
Chord Length (m)	0.125	0.125
Radius (m)	1.875	1.875
Number of blades	3	3
Blade pitch angle (degrees)	-2, 0, 2, 4, 6	-2, 0, 2, 4, 6

2.1.2 Numerical domain

As shown in Figure 2, the simulation domain can be separated into two segments. The part containing the imprint of the VAWT is the round inner domain, which is made to rotate at various TSRs throughout this study. The rectangular part is the outer, stationary domain bounded by the inlet, outlet and walls. Its horizontal walls are modelled as symmetry so that they do not affect the simulation results.

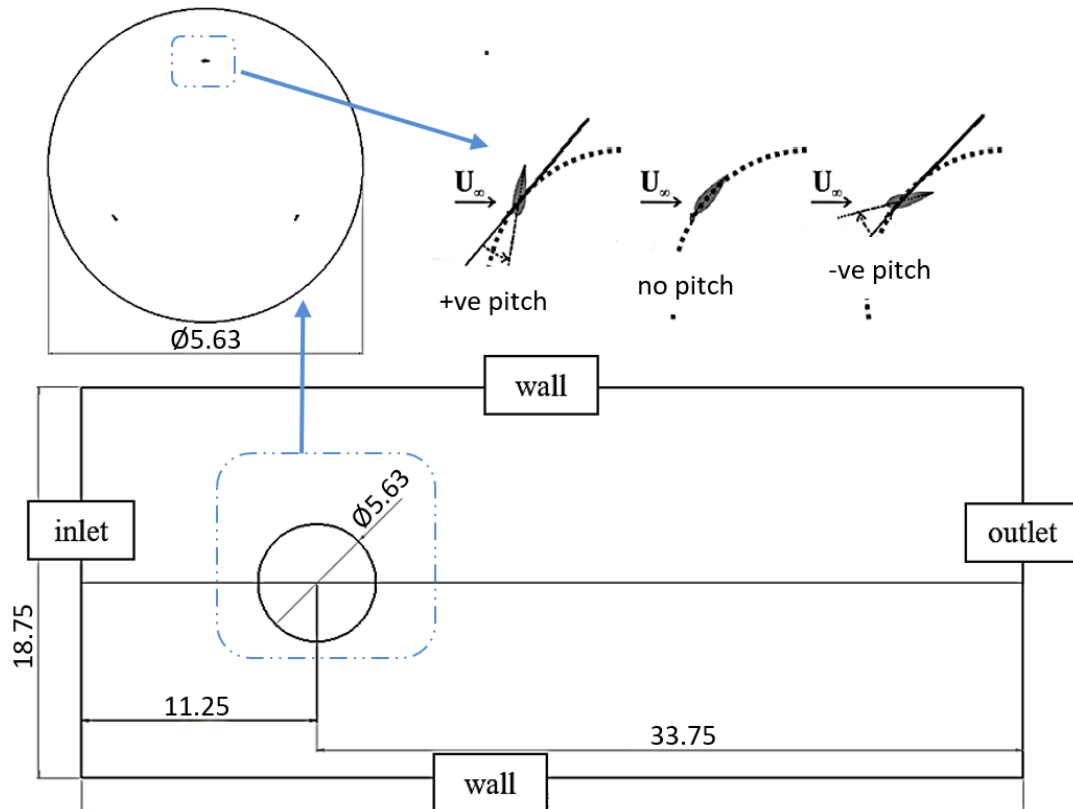


Fig. 2. Inner (top left) and outer (bottom) domains, with schematic showing blade pitch (top right)

All domains were created in Solidworks and then imported over to Ansys as individual parts. The inner domain is 1.5 times the VAWT it incorporates within. This domain is expected to contain a finer mesh, to better capture the immediate flow phenomena surrounding the VAWT. The mesh element size was chosen as a feasible compromise between mesh intensity and adequate capturing of flow around the rotating VAWT. A 3-diameter gap is provided from the centre of the VAWT to the inlet and a further 9-diameter gap to the outlet. These dimensions are adequate for this study as the focus is on calculating the torque generated by the VAWT and not the wake.

2.2 Meshing and Solver Setup

Mesh was generated based on mesh convergence tests, with face sizing that fixed the maximum element size to be 0.05 m for the inner and 0.1 m for the outer domain. To ensure that the boundary layer was well-captured, inflation layers were applied. Initially, 20 layers of inflation were added to the aerofoils, fixing their first layer thickness to be 0.000005 m. However, these inflation layers reduce cell orthogonal quality to unacceptable levels as they produce very high aspect ratio cells.

Edge sizing was applied with at least 1500 divisions to mitigate this issue. Once the flow stabilised for each case, the simulation was paused and then the maximum cell y^+ value was checked for the three aerofoils. If any of the y^+ values were found to be more than 1.5, remeshing is done by reducing the first layer thickness and increasing the number of divisions on the aerofoil edges (to maintain a cell orthogonal quality of more than 0.1). A few snapshots of the meshed domain are presented in Figure 3.

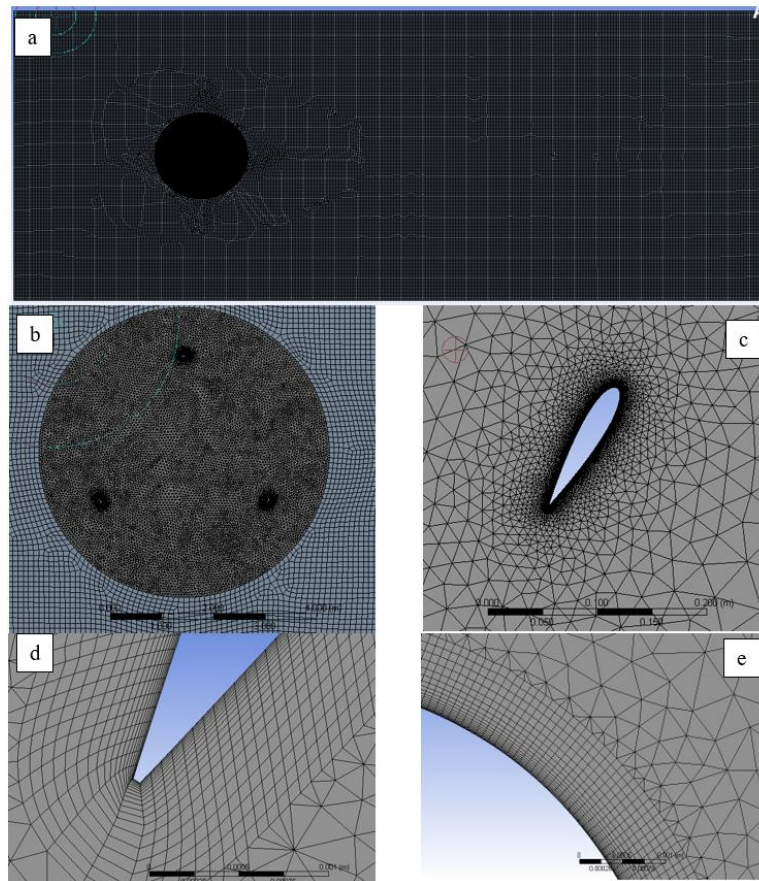


Fig. 3. Meshing: the full domain (a), inner domain (b), around the aerofoil (c), trailing edge (d) and leading edge (e)

Once meshing and naming the appropriate boundaries were concluded, the simulation was set up. A pressure-based, transient, and planar solver was chosen. The $k-\omega$ SST turbulence model was chosen, for its noteworthy performance and widespread usage in similar cases [8]. The boundary conditions were set with the inlet having a 10 m/s incoming velocity, a pressure outlet, and symmetry walls. Given that in all simulated cases, the inlet velocity was fixed at 10 m/s, the TSR was varied only by changing the rotational speed of the inner domain.

The time step of the simulation was set such a way that each subsequent time step captured 1 degree of VAWT rotation. The maximum number of iterations per time step was set at 30, though, for most timesteps, the solution converged well before that. Convergence was determined based on residuals falling below satisfactory levels. The lift, drag and moment coefficient was recorded and plotted onto the screen. Once the flow stabilised, these plots captured repeating patterns, each repeat representing a full revolution, and at least five further cycles were allowed after flow stabilisation. The average co-efficient of the moment was calculated from the last three cycles of the VAWT. The Co-efficient of power was then found by using the relationship that follows:

$$\omega = \frac{2\pi N}{60} \quad (1)$$

$$\lambda = \frac{\omega D}{2V} \quad (2)$$

$$C_p = \frac{P}{\frac{1}{2}\rho AV^3} = \frac{T\omega}{\frac{1}{2}\rho AV^3} = \lambda C_m \quad (3)$$

2.3 Grid Independence Tests

Mesh sensitivity analysis is started with a coarse mesh which was progressively refined from approximately 180,000 elements to 330,000 elements, by which the discrepancy found between progressive results was negligible (less than 1.5%). The number of elements was increased by progressively refining the mesh, first in the stationary domain and then in the inner domain. The result sought here was the moment coefficient, dependent more on the rotary inner domain than the stationary domain, so refinement was started with the outer domain. A face sizing was applied with a default cell size of 0.5 m for the first run, subsequently refining the sizing to 0.1 m, 0.09 m and 0.05 m, respectively. Since the percentage difference between the obtained C_p was negligible to justify any further refinement beyond 0.1 m element size, this size was chosen for the outer domain for all subsequent cases.

The rotary inner domain was next investigated. Here too, face sizing was applied to vary the size of the elements from 1 metre to 0.01 metres. It was observed that refining the mesh beyond an element size of 0.05 m only yielded little change in the average C_p . As such, the element size chosen for the rotary mesh was limited to 0.05 metres for all subsequent simulations. Figure 4 shows the grid convergence graph produced based on the varying number of elements.

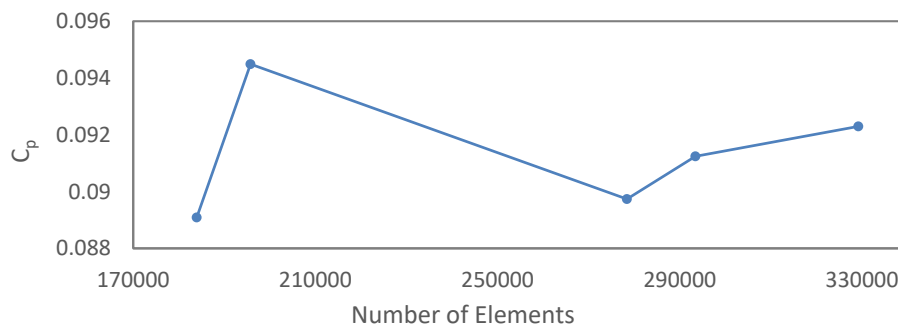


Fig. 4. Average C_p versus number of elements

The second last data point is selected from this graph, as any further refinement of the mesh does not significantly influence the obtained output. For the mesh convergence case, this number of elements is achieved when the inner domain consists of elements sized at 0.05 m and the outer domain has elements sized at 0.1 m, along with 20 inflation layers and edge sizing around the aerofoils to keep the y^+ value below or near 1 (while maintaining the overall cell orthogonal quality to be more than 0.1). Given that the first cell thickness of the inflation layers around the aerofoils is varied for higher TSRs (to maintain y^+ value near to 1) and (therefore) the number of divisions in the mesh surrounding the aerofoils are also accordingly increased (to maintain aspect ratio/cell orthogonal quality), the number of elements varies in subsequent simulations, but the following conditions are maintained in all cases:

- (A) The outer domain has an element of size 0.1 m.
- (B) The Inner domain has an element of size 0.05 m.
- (C) The maximum y^+ values around aerofoils are maintained below or near about 1.
- (D) The cell orthogonal quality is above 0.1.

2.4 Validation

A validation attempt was undertaken with a test case involving the NACA 0018 VAWT with no blade pitch. The finding from the present analysis is compared with existing literature and presented in Figure 5.

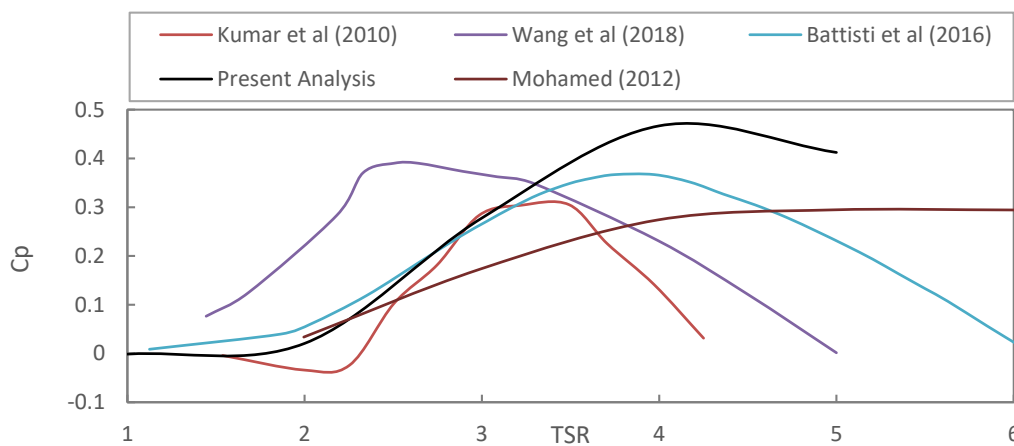


Fig. 5. Graph showing C_p against TSR for the validation case

As can be seen, the model used in this study generally agrees with existing literature except for an overprediction of power-coefficient near TSR 4. The following factors can explain the discrepancies:

- (i) Simplified 2D geometric section: The scope of this study was limited exclusively to 2D simulations, and that too, of only the aerofoil profiles. The struts and the shaft were excluded to ensure a feasible mesh within the limited computational resources available. These could have led to an overprediction of the power-coefficient at higher TSRs [16].
- (ii) Turbulence modelling and solver setup: Different studies utilised different turbulence models and solver setups. Kumar *et al.*, [17] used a CARDAAV model based on the Double Multiple Stream Tube Model (DMST). Mohamed [18] utilised a realisable $k-\epsilon$ turbulence model, which underpredicted the C_p at higher TSRs compared with experimental results during his attempt at validation. This means subsequent results obtained using his validated model may have underpredicted C_p . Battisti *et al.*, [19] used blade element method to compute his results, which closely matches the result obtained in this study until about a TSR of 3.5.
- (iii) The solidity of all simulations performed in this study was kept constant at 0.1. Except for the case with Mohamed [18], all other studies presented here utilised VAWTs with higher solidities ranging between 0.2 and 0.5. Wang *et al.*, [20] for instance, used a VAWT with a solidity of 0.5.

Besides, it should be noted that regardless of how finely the VAWT is modelled and meshed, URANS-based turbulence models can only go so far in terms of accurately predicting VAWT behaviours. Earlier research demonstrates that, 'URANS model delays the occasion of the dynamic stall and overpredicts the tangential force in the upwind zones', and that URANS models are

'insufficient in modelling the large eddies' [21,22]. Despite these factors, the validated model can be accepted, as it predicts results with a level of accuracy that is adequate to compare the two aerofoils and their operations at different blade pitch angles, which is the scope of this study. Also, given that the validation model showed the C_p falls after TSR 4, the scope for all subsequent simulations was set up to a TSR of 4.

3. Results and Discussion

The values of C_p , C_m and velocity & pressure contours for both the aerofoil designs are analysed for various TSR and pitch angles. Figure 6 and Figure 7 show the variation of C_p as the TSR increases at different pitch angles.

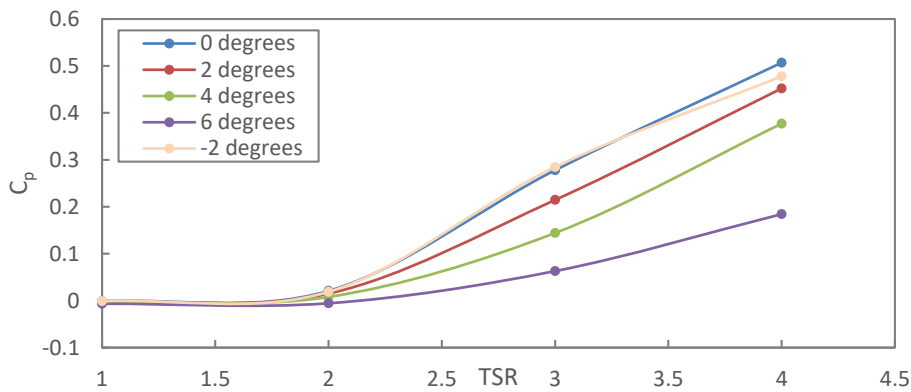


Fig. 6. C_p against TSR at various pitch angles for the VAWT with NACA 0018 aerofoil

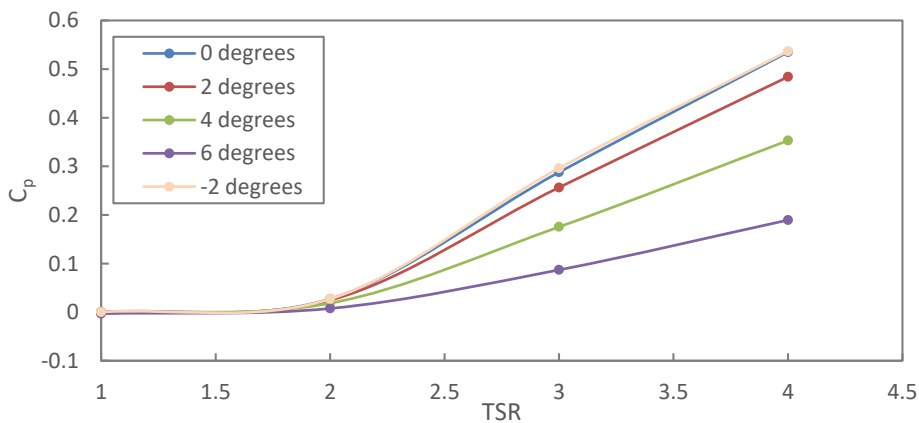


Fig. 7. C_p against TSR at various pitch angles for the VAWT with S1046 aerofoil

As noticed, for all cases, an increase in TSR leads to an increase in the obtained C_p , which is expected. This trend matches well with existing literature, which shows that using the Vortex model, the C_p for 3 bladed VAWTs is expected to rise until the TSR reaches the value of 5 [23]. The increase in C_p was most experienced by VAWTs with a 0-degree blade pitch or with a negative 2-degree blade pitch and least with the 6-degree blade pitch. This trend is further investigated by analysing the pressure and velocity contours of aerofoils at 0 degrees and 6 degrees of pitch, for both the aerofoils. The contours are presented in Figure 8 and Figure 9 at 60-degree intervals of rotation for TSR 4.

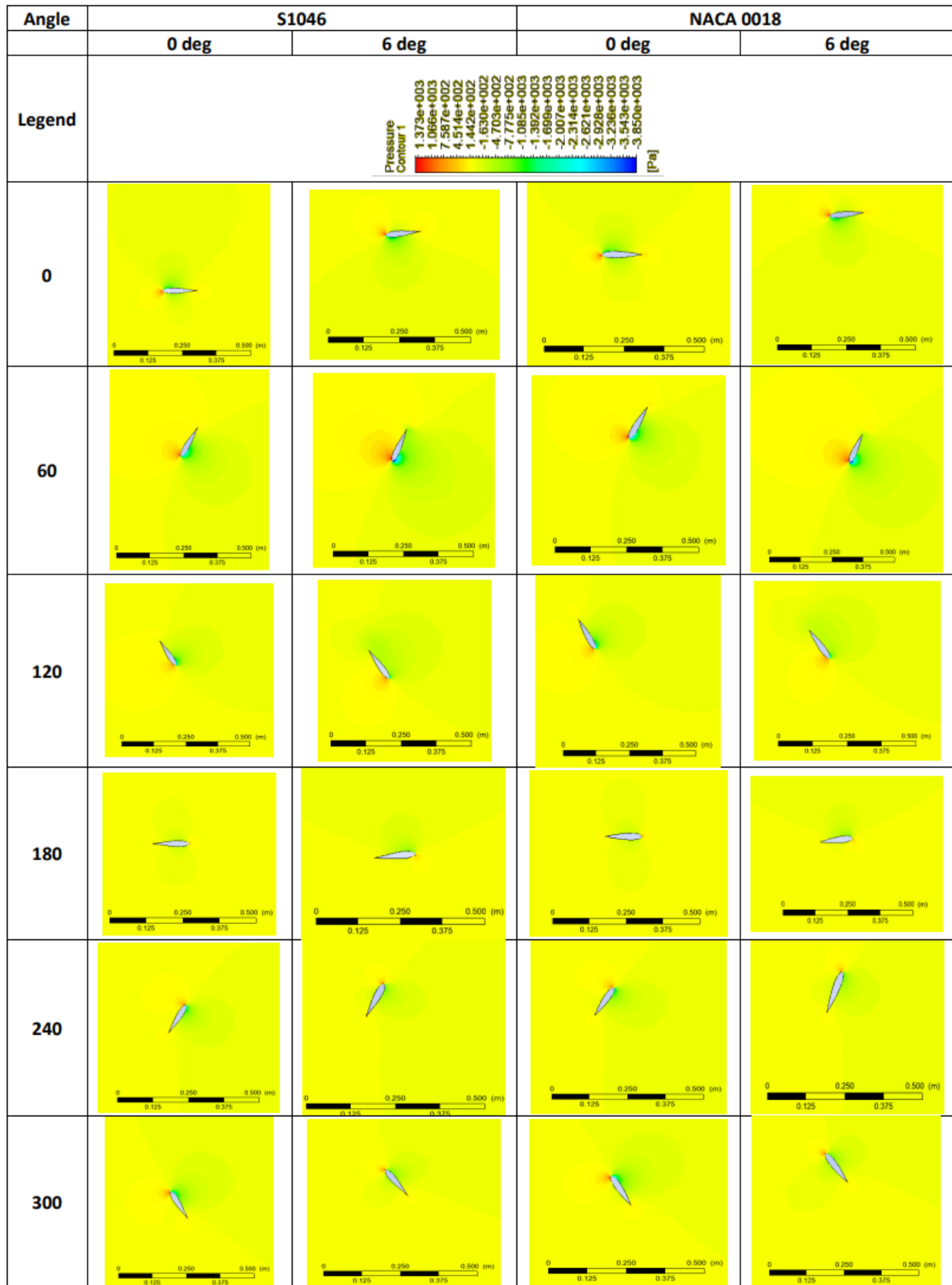


Fig. 8. Contours of pressure for both aerofoil profiles at 0 and 6-degrees of blade pitch, captured at 60 degrees intervals

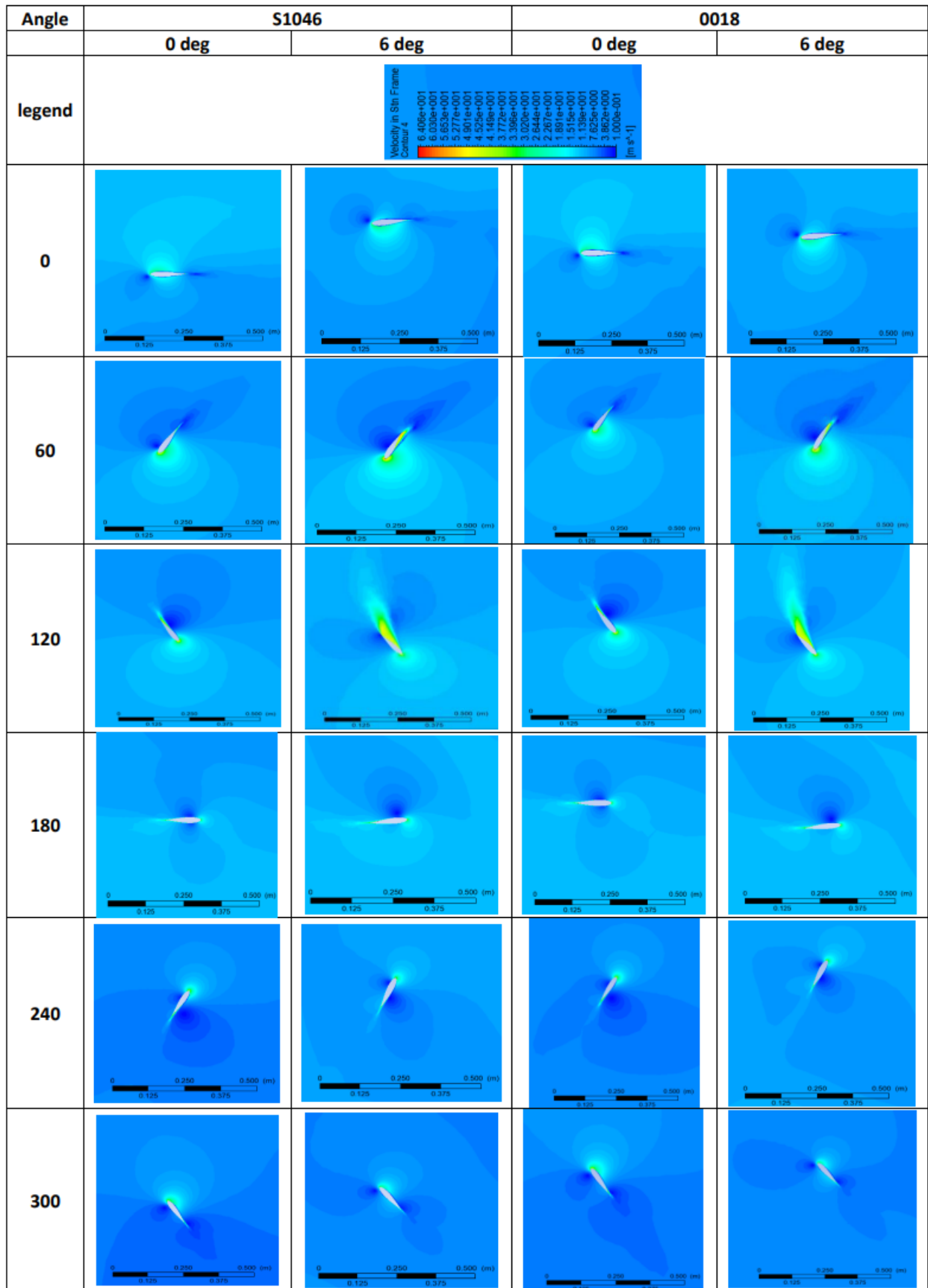


Fig. 9. Contours of velocity for both aerofoil profiles at 0 and 6-degrees of blade pitch, captured at 60-degree intervals

The differences in vortex formation and the onset of dynamic stalls (before flow separation) between the aerofoils with 0 and 6 degrees of blade pitch are evident in the above pressure and velocity contours. Significant discrepancies in flow behaviour due to blade pitch angle are observed for instance at 120-degrees, for both the S1046 and the NACA 0018 aerofoils. With 6 degrees of pitch, the vortex seemed to have travelled far towards the aft of the aerofoil and is being gradually shed, whereby the flows seem more or less attached for the aerofoils with a 0-degree pitch.

Furthermore, comparing plots that follow the C_m generated by a single aerofoil (in Figure 10 and Figure 11) as it undergoes a full rotation (after the flow has stabilised), show that the aerofoils with a 0-degree pitch produce greater positive moment for longer periods of their rotation, and display less abrupt changes in moment generation compared to that of the aerofoils with a 6-degree pitch. Higher positive moment generation and less abrupt flow separation in aerofoils with no/small pitch can explain their higher C_p generation.

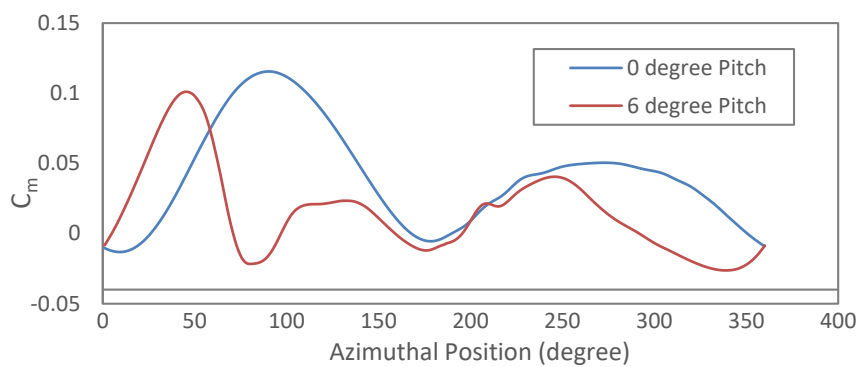


Fig. 10. C_m against azimuthal angle for a single 0018 aerofoil full rotation pitched at 0 and 6 degrees

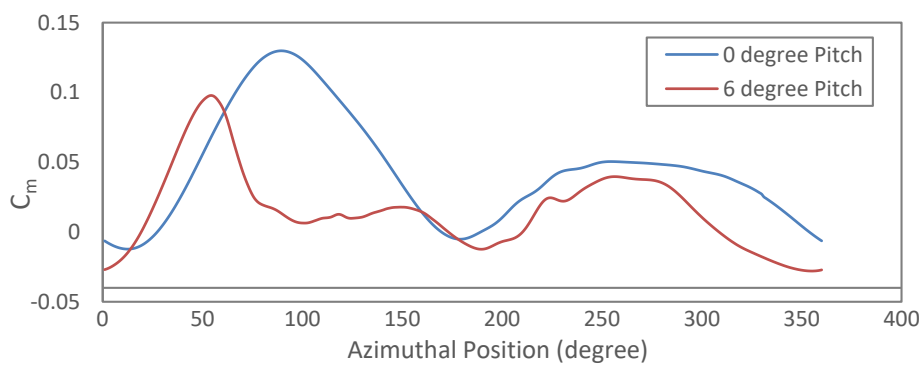


Fig. 11. C_m against azimuthal angle for a single S1046 aerofoil in full rotation at 0 and 6 degrees of blade pitch

For both the S1046 and 0018 blade profiles, the maximum power output occurred at TSR 4. The S0146 aerofoil outperforms the NACA 0018 at all instances except at 4 degrees pitch for TSR 4. The maximum C_p of 0.537 is achieved by the S1046 VAWT when run at TSR 4 and at a blade pitch angle of -2 degrees. The maximum C_p achieved by the NACA 0018 is 0.507 when run with no blade pitch at TSR 4. These results are well observed in Figure 12.

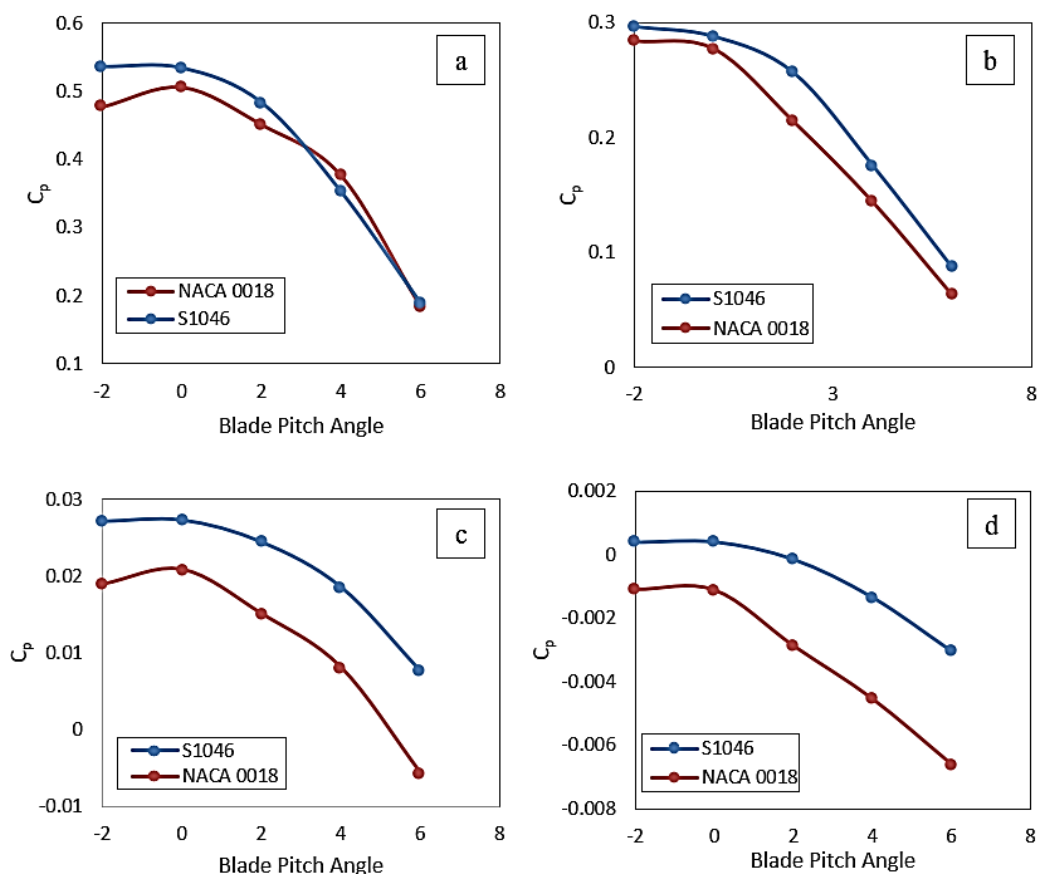


Fig. 12. C_p against blade pitch at (a) TSR 4, (b) TSR 3, (c) TSR 2, (d) TSR 1

4. Conclusion

The paper presents a 2D CFD simulation study which investigate the effects of TSR and blade pitch angle on the performance of VAWTs having two different aerofoil blade profiles: NACA 0018 and S1046. The simulation is performed using the $k-\omega$ SST turbulence model and, it is found that higher TSRs lead to higher power output up to a certain TSR, for both the aerofoil profiles. However, the S1046 aerofoil shows better performance over the NACA 0018 in almost all blade pitch angles and TSRs. This study further concludes that, an optimum VAWT should consist of the S1046 aerofoils with a -2-degree blade pitch to be run at TSR 4. There still remain further avenues to explore, including but not limited to evaluating the performance of various aerofoils at higher solidities (>0.1), using other turbulence models in 3D for performance comparison (at the expense of much superior computational resource requirements). VAWTs with variable blade pitch angles can be investigated as well, which is expected to yield more efficient outcomes. Finally, the self-starting capacity of the VAWTs is another avenue worthy of future exploration.

Acknowledgement

A special thanks to Universiti Teknologi Malaysia (UTM) for the opportunity to carry out the research and the Ministry of Education (MOE) for financial support. This project was supported by Research University Grant-UTM ER [Vot Number: Q.J130000.3851.19J33] initiated by UTM.

References

- [1] Akter, Shamima, Joon Kiat Loo, and Mohammed Abdul Hannan. "Assessing the Impact of Climate Conditions on Harnessing Coastal (Offshore) Wind Energy." In *E3S Web of Conferences*, vol. 65, p. 05010. EDP Sciences, 2018. <https://doi.org/10.1051/e3sconf/20186505010>
- [2] Ariffin, N. I. B., and M. A. Hannan. "Wingsail technology as a sustainable alternative to fossil fuel." In *IOP Conference Series: Materials Science and Engineering*, vol. 788, no. 1, p. 012062. IOP Publishing, 2020. <https://doi.org/10.1088/1757-899X/788/1/012062>
- [3] Brownstein, Ian D., Matthias Kinzel, and John O. Dabiri. "Performance enhancement of downstream vertical-axis wind turbines." *Journal of Renewable and Sustainable Energy* 8, no. 5 (2016): 053306. <https://doi.org/10.1063/1.4964311>
- [4] Eriksson, Sandra, Hans Bernhoff, and Mats Leijon. "Evaluation of different turbine concepts for wind power." *Renewable and Sustainable Energy Reviews* 12 (2008): 1419-1434. <https://doi.org/10.1016/j.rser.2006.05.017>
- [5] Castellani, Francesco, Davide Astolfi, Mauro Peppoloni, Francesco Natili, Daniele Buttà, and Alexander Hirschl. "Experimental vibration analysis of a small scale vertical axis wind energy system for residential use." *Machines* 7, no. 2 (2019): 35. <https://doi.org/10.3390/machines7020035>
- [6] Kadam, A. A., and S. S. Patil. "A review study on Savonius wind rotors for accessing the power performance." *IOSR Journal of Mechanical and Civil Engineering* 5 (2013): 18-24.
- [7] Menter, Florian R. "Two-equation eddy-viscosity turbulence models for engineering applications." *AIAA Journal* 32, no. 8 (1994): 1598-1605. <https://doi.org/10.2514/3.12149>
- [8] Rezaeiha, Abdolrahim, Hamid Montazeri, and Bert Blocken. "On the accuracy of turbulence models for CFD simulations of vertical axis wind turbines." *Energy* 180 (2019): 838-857. <https://doi.org/10.1016/j.energy.2019.05.053>
- [9] Roy, Sukanta, Hubert Branger, Christopher Luneau, Denis Bourras, and Benoit Paillard. "Design of an offshore three-bladed vertical axis wind turbine for wind tunnel experiments." In *International Conference on Offshore Mechanics and Arctic Engineering*, vol. 57786, p. V010T09A046. American Society of Mechanical Engineers, 2017. <https://doi.org/10.1115/OMAE2017-61512>
- [10] Hashem, I., and M. H. Mohamed. "Aerodynamic performance enhancements of H-rotor Darrieus wind turbine." *Energy* 142 (2018): 531-545. <https://doi.org/10.1016/j.energy.2017.10.036>
- [11] Ghazalla, R. A., M. H. Mohamed, and A. A. Hafiz. "Synergistic analysis of a Darrieus wind turbine using computational fluid dynamics." *Energy* 189 (2019): 116214. <https://doi.org/10.1016/j.energy.2019.116214>
- [12] Bohrey, Aayushi, Ramesh Kumar, Aman Thakran, and Hrishita Soni. "Vertical Axis Airborne Wind Turbine: Future of Renewable Energy." In *AIAA Propulsion and Energy 2021 Forum*, p. 3369. 2021. <https://doi.org/10.2514/6.2021-3369>
- [13] Airfoiltools. "Airfoil Tools." *Airfoil Tools*. September 16, 2020. <http://www.airfoiltools.com/>.
- [14] Rezaeiha, Abdolrahim, Hamid Montazeri, and Bert Blocken. "Towards optimal aerodynamic design of vertical axis wind turbines: Impact of solidity and number of blades." *Energy* 165 (2018): 1129-1148. <https://doi.org/10.1016/j.energy.2018.09.192>
- [15] Rezaeiha, Abdolrahim, Ivo Kalkman, and Bert Blocken. "CFD simulation of a vertical axis wind turbine operating at a moderate tip speed ratio: Guidelines for minimum domain size and azimuthal increment." *Renewable Energy* 107 (2017): 373-385. <https://doi.org/10.1016/j.renene.2017.02.006>
- [16] Elkhoury, M., T. Kiwata, and E. Aoun. "Experimental and numerical investigation of a three-dimensional vertical-axis wind turbine with variable-pitch." *Journal of Wind Engineering and Industrial Aerodynamics* 139 (2015): 111-123. <https://doi.org/10.1016/j.jweia.2015.01.004>
- [17] Kumar, Vimal, Marius Paraschivoiu, and Ion Paraschivoiu. "Low Reynolds number vertical axis wind turbine for Mars." *Wind Engineering* 34, no. 4 (2010): 461-476. <https://doi.org/10.1260/0309-524X.3.4.461>
- [18] Mohamed, M. H. "Performance investigation of H-rotor Darrieus turbine with new airfoil shapes." *Energy* 47, no. 1 (2012): 522-530. <https://doi.org/10.1016/j.energy.2012.08.044>
- [19] Battisti, Lorenzo, A. Brighenti, E. Benini, and M. Raciti Castelli. "Analysis of different blade architectures on small VAWT performance." In *Journal of Physics: Conference Series*, vol. 753, no. 6, p. 062009. IOP Publishing, 2016. <https://doi.org/10.1088/1742-6596/753/6/062009>
- [20] Wang, Ying, Sheng Shen, Gaohui Li, Diangui Huang, and Zhongquan Zheng. "Investigation on aerodynamic performance of vertical axis wind turbine with different series airfoil shapes." *Renewable Energy* 126 (2018): 801-818. <https://doi.org/10.1016/j.renene.2018.02.095>
- [21] Li, Chao, Songye Zhu, You-lin Xu, and Yiqing Xiao. "2.5 D large eddy simulation of vertical axis wind turbine in consideration of high angle of attack flow." *Renewable Energy* 51 (2013): 317-330. <https://doi.org/10.1016/j.renene.2012.09.011>

- [22] Ferreira, CJ Simao, H. Bijl, G. Van Bussel, and G. Van Kuik. "Simulating dynamic stall in a 2D VAWT: modeling strategy, verification and validation with particle image velocimetry data." In *Journal of Physics: Conference Series*, vol. 75, no. 1, p. 012023. IOP Publishing, 2007. <https://doi.org/10.1088/1742-6596/75/1/012023>
- [23] Dumitrache, Alexandru, Florin Frunzulica, Horia Dumitrescu, and Bogdan Suatean. "Influences of some parameters on the performance of a small vertical axis wind turbine." *Renewable Energy and Environmental Sustainability* 1 (2016): 16. <https://doi.org/10.1051/rees/2016024>